



Chemistry A European Journal

 **Chemistry
Europe**
European Chemical
Societies Publishing

Accepted Article

Title: Exciton Transport in Molecular Semiconductor Crystals for Spin-Optoelectronics Paradigm

Authors: Weigang Zhu, Yajing Sun, Jie Liu, Shuming Bai, Zhicheng Zhang, Qiang Shi, Wenping Hu, and Hongbing Fu

This manuscript has been accepted after peer review and appears as an Accepted Article online prior to editing, proofing, and formal publication of the final Version of Record (VoR). This work is currently citable by using the Digital Object Identifier (DOI) given below. The VoR will be published online in Early View as soon as possible and may be different to this Accepted Article as a result of editing. Readers should obtain the VoR from the journal website shown below when it is published to ensure accuracy of information. The authors are responsible for the content of this Accepted Article.

To be cited as: *Chem. Eur. J.* 10.1002/chem.202003447

Link to VoR: <https://doi.org/10.1002/chem.202003447>

WILEY-VCH

Exciton Transport in Molecular Semiconductor Crystals for Spin-Optoelectronics Paradigm

Weigang Zhu,^{*,†} Yajing Sun,[†] Jie Liu, Shuming Bai, Zhicheng Zhang, Qiang Shi, Wenping Hu,^{*} and Hongbing Fu^{*}

Abstract: Organic semiconductors with long-range exciton diffusion length is highly desirable for optoelectronics but currently remain rare. Here, we show the estimated diffusion length of singlet excitons (L_D) in 2,6-diphenyl anthracene (DPA) crystals grown by solvent evaporation is up to ~ 124 nm. These crystals show a previously unseen parallelogram morphology with layer-by-layer edge-on molecular stacking, isotropic optical waveguiding, radiation rate and non-radiation rate constants of 0.15 ns^{-1} and 0.26 ns^{-1} respectively, as well as good field-effect transistor hole mobility and theoretically computed strong electronic couplings as high as 109 meV . Photoresponse experiments reveal that the photoconductivity of DPA crystals is surprisingly not related to the radiative pathway, but associated with rapid exciton diffusion to crystal surface for charge separation and carrier bimolecular recombination. Taken together, this study shows that DPA is a promising semiconducting material for new organic optoelectronics paradigm.

Organic optoelectronic science and technology have attracted worldwide interests due to their potentials to offer flexible, stretchable electronic device products that is complementary to other traditional commercial semiconductor techniques, therefore efficiently create social and economic benefits. This novel interdisciplinary is located at the interface between chemistry, physics, chemical engineering, and materials science and engineering. Organic optoelectronics involves π -conjugated polymer and small molecule as the core materials via chemical synthesis, towards targeted applications including optical data storage, optical switch,^[1] laser,^[2] light-emitting diode (LED),^[3] thin film transistor (TFT),^[4] and solar cell,^[5] etc. From the perspective of chemists, polymers are different from batch-to-batch synthesis, difficult to scale-up produce in industry (e.g. NF300^[5], and N2200), and generally show low crystallinity. From

the perspective of physicists, despite of some efforts on P3HT,^[6] polymers are still too complex to be understood, both in structure, morphology and device applications. In sharp contrast, small molecules have many advantages. They have certain chemical structures, are easy to chemically modify, highly crystalline, as well as show high electronic device metrics (e.g. ITIC, and Y6).^[7-8] Moreover, small molecule semiconductors such as α,ω -bis(biphenyl)terthiophene,^[9] 2-(4-hexylphenylvinyl)anthracene,^[10] and oligo(*p*-phenylenevinylene)^[11] show strong photoluminescence (PL) with high photoluminescence quantum yield (PLQY) up to 90%^[12] in solid state. For solution processing, molecular semiconductors with multi-functions can be directly printed into large-area devices.^[13] Therefore, molecular semiconductors are a new class of carbon-based materials which are desirable in optoelectronics.^[14] Among many molecular semiconductors, anthracene and its derivatives are particularly interesting, due to their unique high charge carrier mobility (μ) and high PLQY simultaneously. We have been working in this research area since 2009,^[15] and have reported several high-performance anthracene derivatives and corresponding device applications in TFT, LED, and light-emitting transistor (LET),^[14, 16-17] but the underlying mechanism for such interesting properties remains unclear, and the understanding of their excitons behavior is also still in its fancy.^[14]

Photo/electrically-generated exciton in molecular semiconductors is known to play the key role in their resulted optoelectronic and catalysis properties, one of the specific parameters, exciton diffusion length (L_D), is used to quantitatively determine specific applications. For organic solar cells, the photoactive layer materials generally show L_D of 10-20 nm,^[18] and this allows excitons to separate into free charge efficiently within microscopic phase segregated domains of bulk-heterojunction films.^[19] For some single crystals exhibiting singlet fission, L_D of triplets can surprisingly reach several micrometres (μm) for good photoconductivity performance.^[20] On the other hand, the experimentally determined L_D values of organic semiconductors are largely varied using different methods (such as PL mapping,^[21-23] PL quenching, and photoconductivity) in literature,^[24-25] and the correlations between L_D and device parameters are still lacking, which is highly interested within optoelectronics research community.

Herein, by using 2,6-diphenyl anthracene (DPA) as prototype, we report that the estimated L_D of singlet excitons in DPA crystals is up to 124 nm. The DPA single crystals are grown by tetrahydrofuran (THF) solvent evaporation, and show a new parallelogram crystal morphology with edge-on molecular orientation relative to substrate. Steady and time-resolved PL spectroscopy measurements reveal that DPA crystals show isotropic optical waveguiding property, PL lifetime (τ) of 2.45 ns, radiation rate constant (k_r) of 0.15 ns^{-1} , and non-radiation rate constant (k_{nr}) of 0.26 ns^{-1} , respectively. Field-effect transistor (FET) measurements show that DPA crystals have good hole mobility (μ_h) of $\sim 2 \text{ cm}^2 \text{ V}^{-1} \text{ s}^{-1}$ in ambient, which is supported by

[a] W. Zhu,^[†] J. Liu, S. Bai, Prof. Q. Shi, Prof. W. Hu, Prof. H. Fu
Institute of Chemistry, Chinese Academy of Science (ICCAS), Beijing
National Laboratory for Molecular Sciences (BNLMS)
Beijing, 100190, China
E-mail: zhuweigang@iccas.ac.cn (W.Z.); hongbing.fu@iccas.ac.cn (H.F.)

W. Zhu, J. Liu, S. Bai
University of Chinese Academy of Sciences (UCAS)
Beijing, 100049, China

Dr. Y. Sun,^[†] Prof. Z. Zhang, Prof. W. Hu
Department of Chemistry, School of Science, Tianjin Key Laboratory of
Molecular Optoelectronic Sciences (TJ-MOS), Tianjin University (TJU)
Tianjin, 300072, China
E-mail: huyw@tju.edu.cn (W.H.)

[†] These two authors contributed equally to this work.

[b] This work was supported by the National Natural Science Foundation of China (No. 20925309, 21190034, 21073200, 21073079, J1103307), the National Basic Research Program of China (973) 2011CB808402, 2012CB933102, the Specialized Research Fund for the Doctoral Program of Higher Education (SRFDP, 20110211130001) and the Fundamental Research Funds for the Central Universities and 111 Project. Weigang would like to thank his parents for support over years on the occasion of their near 70 years' birthday, and wish them all the best, happiness, joy, and health.

Supporting information for this article is available from the author or via a link at the end of the document.

single-crystal-structure based computed large electronic couplings. It will be seen that these allow good photoconductivity response of DPA crystals, but very slow current decay in the photo-switch experiment. Unexpectedly, the photoconductivity is not related to the radiative process, but is associated with the dynamics that laser-induced singlet excitons rapidly diffuse to crystal surface for charge separation and carrier bimolecular recombination (BR). The L_D together with device mechanisms and "structure-mobility-exciton-property" correlations show that DPA has the potential to open up a new spin-optoelectronics paradigm.

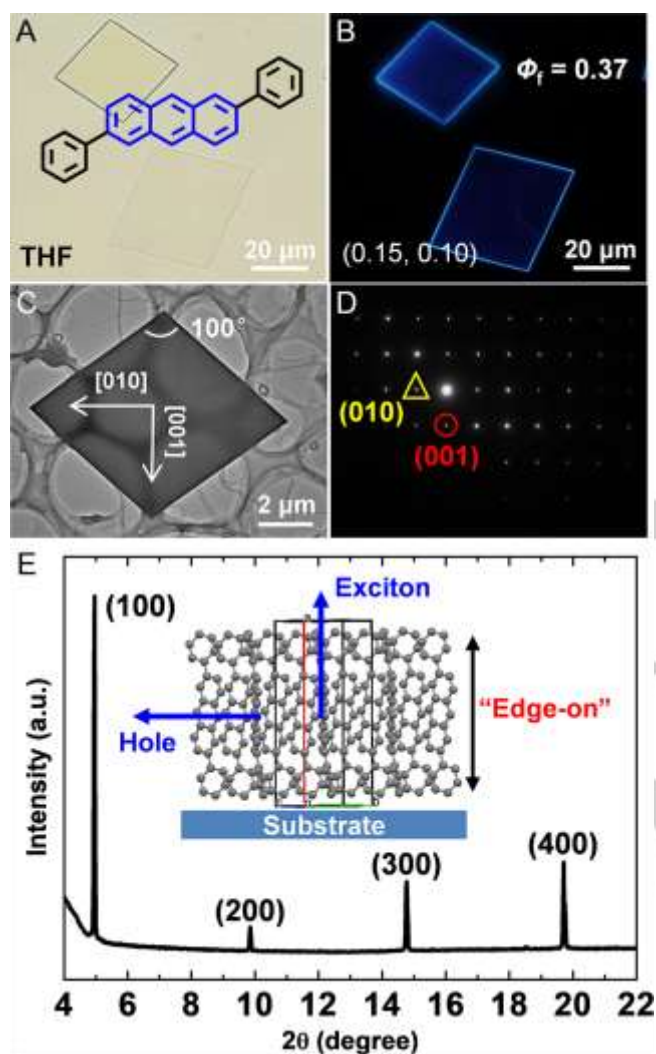


Figure 1. DPA crystal and structure. (A) Optical and (B) PL images of DPA crystals; (C) TEM, (D) SAED images, and (E) XRD pattern of crystal.

DPA crystals were grown by a solvent evaporation method. In a typical experiment, material was completely dissolved in THF, and the solution was dropped onto substrate, crystals then appeared after THF was slowly evaporated. DPA crystals show thin and large size up to hundreds of μm (Figure 1A, S1), and a new parallelogram shape different from that obtained from physical vapour transport (PVT) method^[14]. This crystal morphology difference can be explained by Materials Studio software simulation (Figure S2). The computed result shows that DPA has a stable hexagon morphology but a potential metastable parallelogram crystal shape. Compared with PVT

method, the nucleation and growth process of DPA crystal nucleus under THF evaporation is rapid, thus leading to the formation of a metastable parallelogram morphology. DPA crystals show strong blue PL at CIE coordinate of (0.15, 0.10) (Figure S3) with measured PLQY (Φ_f) of 0.37 (Figure 1B), agreeing well with our previous data of powder.^[14]

Transmission electron microscopy (TEM), selected area electron diffraction (SAED), and X-ray diffraction (XRD) experiments were performed to determine the single crystal structure. Typical TEM image (Figure 1C, S4) and corresponding SAED pattern (Figure 1D) on individual DPA crystal reveal its single crystalline nature. The measured d -space of 7.81 Å and 6.59 Å in nice electron diffraction patterns are indexed to (010) and (001), respectively, compared with our previously deposited cif structure: $a = 17.973$ Å, $b = 7.352$ Å, $c = 6.245$ Å, $\alpha = 90.00^\circ$, $\beta = 90.646^\circ$, $\gamma = 90.00^\circ$ (CCDC no. 1044209, Figure S5).^[26] Note that interestingly, these results are in accord well with the Materials Studio software simulations. Typical XRD curve of DPA crystals *in-situ* grown on clean glass substrate (Figure 1E) shows very strong (h00) peaks, indicating that DPA molecules are "edge-on" orientated relative to substrate with in-plane intermolecular π -electronic couplings and they are layer-by-layer stacked to form ~100 nm to several μm thick crystals, as measured by Atomic Force Microscopy (Figure S6). Importantly, this unique molecular packing of DPA crystal is perfect for in-plane charge transport in the FET configuration, which should yield good charge carrier mobility (*vide infra*).

Photophysical parameters of DPA were firstly characterized. DPA monomer in THF shows well-structured absorption and PL spectra, but interestingly 0-0 absorption peak of monomer shows lower oscillator strength (f) compared with 0-1 and 0-2 absorption. The Φ_f of monomer in THF is 0.66 referred to 9,10-diphenyl anthracene. For the 0-0 PL peak of crystals (Figure 2A), it shows lower f due to significant self-absorption of a large quantity of crystals in the experiments. The PL decay lifetime (τ) of monomer and crystal determined on a streak camera are 4.29 ns and 2.45 ns (Figure 2B), respectively. To further quantify the radiation pathway of S_1 to S_0 (Figure 4B), the radiation rate constant (k_f) is calculated to be 0.15 ns^{-1} (Table 1) by using the equation:^[27]

$$k_f = \Phi_f / \tau$$

This value is mild among the reported values from single crystals of organic materials.^[28] The corresponding non-radiation rate constant (k_{nr}) is 0.26 ns^{-1} , by using the equation:^[25, 28]

$$\Phi_f = k_f / (k_f + k_{nr})$$

To better understand the photophysical properties, the electronic structures and vibrational properties of ground state and excited state in solid DPA were obtained by first principles calculation. Considering the aggregation effects, we adopt the hybrid Quantum Mechanics/Molecular Mechanics (QM/MM) method, selecting one central DPA molecule as the high-precision layer with (TD) DFT calculation. And for the surrounding molecules, we use the low-precision molecular dynamics with Universal Force Field (UFF) force field (Figure S7). After optimizing completely, we calculate the vertical (E_{ver}) and adiabatic excitation energy (E_{ad}) of DPA molecule, $E_{\text{ver}} = 3.02 \text{ eV}$ and $E_{\text{ad}} = 2.85 \text{ eV}$, respectively, as shown in Figure 2E. By analyzing the properties of excited states, we find the transition process with the maximum oscillator strength f happens in the 0-0 transition, $f_{0-0} = 0.18$, while interestingly $f_{0-1} = 0.002$. With the

help of thermal vibration correlation function, the calculated emission spectrum is shown in **Figure 2F** and the 0-0 emission peak is around 450 nm, which are consistent well with the experimental results from DPA crystals. The calculated radiative transition rate k_r is 0.053 ns^{-1} and the internal conversion transition rate k_{ic} is 0.0148 ns^{-1} , much lower the experimental values (**Table 1**). In contrast, the calculated Φ_f is 0.78, higher than the experiment value of 0.37. Overall, the photophysical computations rationalize the strong PL property of DPA.

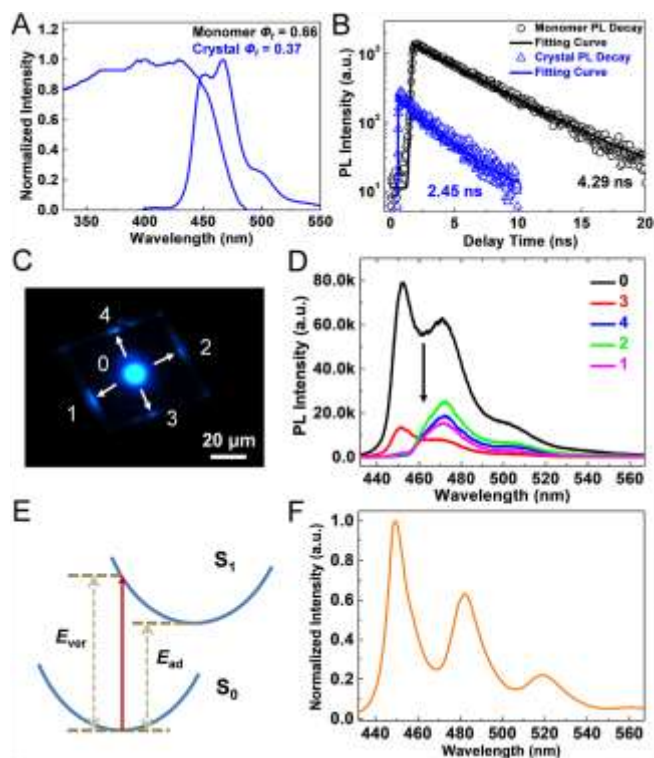


Figure 2. Photophysical properties and computation. (A) Diffuse absorption spectrum of DPA powder and PL spectrum of DPA crystals; (B) PL decay of monomer and crystals; (C) Typical PL image of an individual DPA crystal and (D) corresponding PL spectra under 408 nm laser excitation; (E) The transition process scheme for DPA; (F) The calculated fluorescence spectrum.

Moreover, micro-area photoluminescence (μ -PL) measurements^[27] were performed to spatially investigate PL propagation and optical waveguiding properties in individual DPA crystal (**Figure 2C, S8**). Under the excitation of a $\lambda = 408 \text{ nm}$ laser, the generated PL propagates and out-couples along four directions to crystal edges with similar optical loss, leaving similar PL intensity at the crystal edges (**Figure 2D**). This “isotropic” optical waveguiding property of DPA is consistent with our and other groups’ observations on organic molecular crystals.^[27, 29] Note that both of the PL propagation directions are almost parallel to crystal edges and not related to the molecular packing structure. The collected PL intensity and optical waveguiding property is not influenced by applied voltage bias even up to 100 V (**Figure S9**), indicating exciton behavior is not affected by electric field, and this would be very interesting in other electronic device operations, such as solar cell and LET.

Charge carrier mobility of DPA crystals was studied by using a bottom-gate top-contact FET configuration (**Figure 3A**). Gold (Au) was selected as the source (S) and drain (D) electrode material. FET devices were fabricated using the home-developed “copper grid mask” method,^[30] and gold electrode

was thermally evaporated (**Figure S10**). The typical transfer and output curves of DPA crystal FET device are shown in **Figure 3B,C**, respectively. The μ_h calculated in the saturation region is $2.26 \text{ cm}^2 \text{ V}^{-1} \text{ s}^{-1}$, and the maximal mobility obtained is $2.41 \text{ cm}^2 \text{ V}^{-1} \text{ s}^{-1}$ at ambient conditions. The average μ_h value collected from 10 separated devices is $1.92 \pm 0.38 \text{ cm}^2 \text{ V}^{-1} \text{ s}^{-1}$, much lower than the result grown from PVT method, which is known to provide very high single crystal quality with thin thickness.^[31] However, the threshold voltage (V_T) herein is $> -20 \text{ V}$, consistent with our previous observation from PVT grown crystal based FETs.^[14] The unusual large V_T reflects intrinsic different charge transport property of DPA from other common organic semiconductors in FET geometry, thus DPA is a special class of material that deserves further studies of charge transport physics.

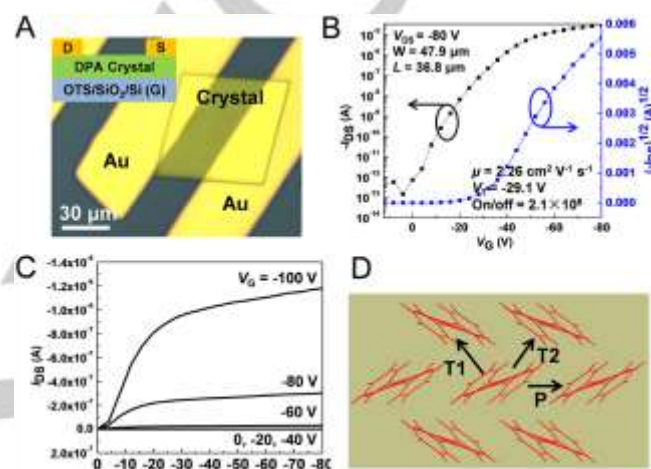


Figure 3. FET carrier mobility and electronic couplings. (A) Typical optical image of a DPA crystal FET; (B) Typical transfer and (C) corresponding output characteristics of a DPA crystal FET; (D) Molecular packing in DPA crystal.

Table 1. Optoelectronic properties of DPA single crystals.

Φ_f	τ (ns)	k_f (ns^{-1})	k_{nr} (ns^{-1})	μ_h [a] ($\text{cm}^2 \text{ V}^{-1} \text{ s}^{-1}$)	L_D (nm)	c
0.37	2.45	0.15	0.26	1.92 ± 0.38	123.63	0.57

[a] Average with one standard deviation (1σ) is taken over 10 separate devices.

Theoretical computations were performed to understand the charge carrier transport properties. The DPA molecules pack in a herringbone fashion similar to most anthracene derivants, so we define the electronic couplings of charge transfer accordingly, as shown in **Figure 3D**. The coupling values T_1 , T_2 , P of DPA crystals are computed to be 109, 109, and 18 meV (**Table S1**), respectively. Although the computation methods are slightly different, the T_1 and T_2 are surprisingly much higher than those of pentacene (79, 45 meV)^[32] and hexacene (88, 60 meV),^[33] suggesting that DPA is a potential high-mobility semiconductor, while the reorganization energy (λ) of DPA is 143 meV, much higher than that of pentacene (95 meV),^[32] and Hexacene (79 meV).^[33] This may compromise the final charge carrier mobility of DPA single crystals (**Table 1**).

The L_D plays the central role in organic optoelectronic devices, however, there is limited study on L_D of organic

semiconductor crystals.^[20, 25, 34-35] The L_D here is roughly calculated using the equation previously used for perovskite semiconductors which we believe is not perfect for organics but indeed a best-case method.^[36]

$$L_D = \sqrt{\frac{k_B T}{e} \times \mu \times \tau}$$

Where μ is exciton mobility (here we assume as FET hole mobility, note that the hole mobility can be much lower than the mobility of singlet excitons, so the real L_D would be higher), τ is exciton lifetime (here is PL decay lifetime), k_B is Boltzmann's constant, and T is the sample temperature. Using this method and equation, the obtained L_D s are estimated values but these do not change the final understandings on the material. Unexpectedly, using the values we measured from FET and streak camera, the L_D of DPA crystal is 123.63 nm. By applying the mobility value of $34 \text{ cm}^2 \text{ V}^{-1} \text{ s}^{-1}$ we obtained previously,^[14] L_D is calculated to be as high as 464 nm, among the good values of singlet exciton in organic semiconductors,^[25, 37] but much shorter than those of perovskite bulk crystals ($L_D > 10 \mu\text{m}$).^[36] The singlet exciton transport with high μ_h and strong PL property of DPA, which is limited presented in the organic electronic material family,^[21, 34] should provide an ideal platform for advanced optoelectronics, such as efficient solar electricity, LET, spintronic device, and even electrically-pumped lasing.

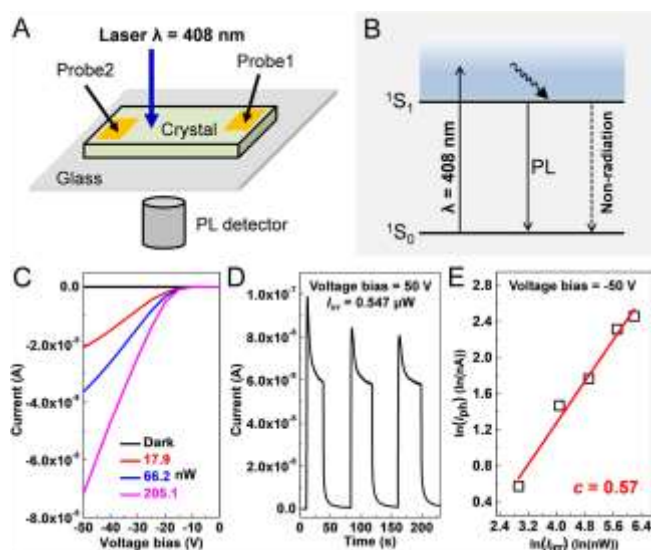


Figure 4. Photoconductivity measurements. (A) Schematic diagram of μ -PL and photoconductivity integrated platform; (B) Photophysics model of DPA crystal; (C) Typical I - V characteristics of DPA crystal based devices under different I_{irr} s of $\lambda = 408 \text{ nm}$ excitation laser; (D) Corresponding on/off switch curve; (E) Typical dependence of $\ln(I_{ph})$ on $\ln(I_{irr})$ of DPA crystal device.

With these understandings on L_D of DPA crystals, we therefore performed photoconductivity measurements. DPA single crystals were grown by solvent evaporation, and devices were *in-situ* fabricated using the same procedure as FET. Photoresponse measurements were conducted on a home-developed optoelectronic characterization platform^[30] that allows to simultaneously probe electronic and photonic signals of samples at micro-nanoscale (Figure 4A). Indeed DPA crystal shows strong photoresponse to the excitation laser ($\lambda = 408 \text{ nm}$), and significant enhancement of current is determined under the

intensity of only tens of nW (Figure 4C). This is understandable in terms of L_D vs crystal thickness, which allows photogenerated free charge carriers quickly move to electrodes. Surprisingly, the collected μ -PL intensity does not change when measuring photoconductivity (Figure S16), contrary to the previous photoconductivity experiments on rubrene crystal where triplet excitons are involved.^[20] In DPA crystals, the radiation pathway is not related to the free charge carrier photogeneration, which eliminates the possibility that DPA crystal shows singlet exciton fission. Therefore, the non-radiation processes from 1S_1 to 1S_0 (k_{nr}) play the key role in the measured photoconductivity (Figure 4B, 2B).

In a typical photo-switch experiment, with a voltage bias of 50 V and laser excitation intensity of 0.547 μW , DPA crystal device shows rapid current increase to “on” state, while drop to a stable state very slowly (tens of seconds) with a current decay, but the overall current on/off ratio remains significant (Figure 4D). This slow current decay suggests that large numbers of free charge carriers are existed after the laser excitation immediately, but also suffer significant recombination due to the high carrier density. To further quantify the hole-electron recombination, the photocurrent I_{ph} under different laser excitation intensities (I_{irr}) is measured, using the equation:^[38]

$$I_{ph} = I_{illum} - I_{dark}$$

where I_{illum} is the current under laser excitation, and I_{dark} is the current detected under dark. Using the equation:^[38]

$$I_{ph} \sim (I_{irr})^c$$

the photocapture coefficient (c) can be extracted from the $\ln(I_{ph}) \sim \ln(I_{irr})$ curve. The typical $\ln(I_{ph}) \sim \ln(I_{irr})$ curve of DPA crystal device exhibits linear relation (Figure 4E), and the c is fitted to be 0.57, which suggests BR mechanism at the surface of DPA crystal. This is consistent with L_D and crystal thickness, and long-lived excitons rapidly diffuse across the layer-by-layer “edge-on” stacked DPA molecules to the surface of crystal, and separate into free charge carrier, transport, and recombination for conductivity (Figure 1E), although for this effect no long L_D is required. Overall, the crystal surface plays an important role in charge separation and recombination for photoconductivity, similar to our previous observations on long L_D materials.^[38]

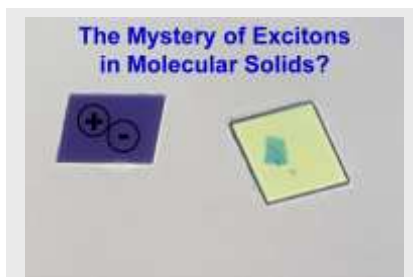
In conclusion, single crystals of DPA have been grown by a simple solution evaporation method. DPA crystals show a previously unseen parallelogram morphology, isotropic optical waveguiding property, radiation rate and non-radiation rate constants of 0.15 ns^{-1} and 0.26 ns^{-1} respectively, good in-plane μ_h of $\sim 2 \text{ cm}^2 \text{ V}^{-1} \text{ s}^{-1}$, estimated L_D of 124 nm, unique slow photoconductivity switching, and photocapture coefficient of 0.57. The L_D and good μ_h are consistent with the photocurrent decay and crystal surface BR mechanism in the photoconductivity experiments. Computed strong electronic couplings and relatively large reorganization energy explain the good μ_h in ambient conditions, and interestingly the simulated PL spectrum and strong Φ_f agree well with the experimental observations. The L_D and “molecular packing-mobility-exciton-property” relations here together show that DPA is a potential semiconductor to open up a new optoelectronics paradigm. Further related research, underway in our Laboratory, are printing flexible, stretchable, large-area carbon-based semiconducting material devices and circuits, developing ultrafast time-resolved electron paramagnetic resonance (*tr*-EPR) spectroscopy to probe unseen high spin state and dynamics, as

well as exploring their applications in organic quantum information science (OQIS).

Keywords: crystal • charge mobility • exciton • computational chemistry • photoconductivity

- [1] W. Zhu, L. Zhu, L. Sun, Y. Zhen, H. Dong, Z. Wei, W. Hu, *Angew. Chem. Int. Ed.* **2016**, *55*, 14023-14027.
- [2] I. D. Samuel, G. A. Turnbull, *Chem. Rev.* **2007**, *107*, 1272-1295.
- [3] X. Ai, E. W. Evans, S. Dong, A. J. Gillett, H. Guo, Y. Chen, T. J. H. Hele, R. H. Friend, F. Li, *Nature* **2018**, *563*, 536-540.
- [4] Z. Ni, H. Wang, Q. Zhao, J. Zhang, Z. Wei, H. Dong, W. Hu, *Adv. Mater.* **2019**, *31*, e1806010.
- [5] W. G. Zhu, J. M. Alzola, T. J. Aldrich, K. L. Kohlstedt, D. Zheng, P. E. Hartnett, N. Eastham, W. Huang, G. Wang, R. M. Young, G. C. Schatz, M. R. Wasielewski, A. Facchetti, F. S. Melkonyan, T. J. Marks, *ACS Energy Lett.* **2019**, *4*, 2695-2702.
- [6] M. Alizadehaghdam, S. Siegenführ, F. Abbasi, G. Reiter, *Journal of Polymer Science Part B: Polymer Physics* **2019**, *57*, 431-437.
- [7] C. Wang, H. Dong, L. Jiang, W. Hu, *Chem. Soc. Rev.* **2018**, *47*, 422-500.
- [8] Y. Yuan, G. Giri, A. L. Ayzner, A. P. Zoombelt, S. C. Mannsfeld, J. Chen, D. Nordlund, M. F. Toney, J. Huang, Z. Bao, *Nat. Commun.* **2014**, *5*, 3005.
- [9] K. Sawabe, M. Imakawa, M. Nakano, T. Yamao, S. Hotta, Y. Iwasa, T. Takenobu, *Adv. Mater.* **2012**, *24*, 6141-6146.
- [10] A. Davdand, A. G. Moiseev, K. Sawabe, W.-H. Sun, B. Djukic, I. Chung, T. Takenobu, F. Rosei, D. F. Perepichka, *Angew. Chem. Int. Ed.* **2012**, *51*, 3837-3841.
- [11] H. Nakanotani, M. Saito, H. Nakamura, C. Adachi, *Appl. Phys. Lett.* **2009**, *95*, 033308.
- [12] H. Nakanotani, R. Kabe, M. Yahiro, T. Takenobu, Y. Iwasa, C. Adachi, *Appl. Phys. Express* **2008**, *1*, 091801.
- [13] H. Minemawari, T. Yamada, H. Matsui, J. y. Tsutsumi, S. Haas, R. Chiba, R. Kumai, T. Hasegawa, *Nature* **2011**, *475*, 364.
- [14] J. Liu, H. Zhang, H. Dong, L. Meng, L. Jiang, L. Jiang, Y. Wang, J. Yu, Y. Sun, W. Hu, A. J. Heeger, *Nat. Commun.* **2015**, *6*, 10032.
- [15] L. Jiang, W. Hu, Z. Wei, W. Xu, H. Meng, *Adv. Mater.* **2009**, *21*, 3649-3653.
- [16] A. Davdand, A. G. Moiseev, K. Sawabe, W. H. Sun, B. Djukic, I. Chung, T. Takenobu, F. Rosei, D. F. Perepichka, *Angew. Chem. Int. Ed.* **2012**, *51*, 3837-3841.
- [17] J. Li, K. Zhou, J. Liu, Y. Zhen, L. Liu, J. Zhang, H. Dong, X. Zhang, L. Jiang, W. Hu, *J. Am. Chem. Soc.* **2017**, *139*, 17261-17264.
- [18] W. Zhu, A. P. Spencer, S. Mukherjee, J. M. Alzola, V. K. Sangwan, S. H. Amsterdam, S. M. Swick, L. O. Jones, M. C. Heiber, A. A. Herzog, G. Li, C. L. Stern, D. M. DeLongchamp, K. L. Kohlstedt, M. C. Hersam, G. C. Schatz, M. R. Wasielewski, L. X. Chen, A. Facchetti, T. J. Marks, *J. Am. Chem. Soc.* **2020**, *142*, 14532-14547.
- [19] J. Heeger Alan, *Adv. Mater.* **2013**, *26*, 10-28.
- [20] H. Najafov, B. Lee, Q. Zhou, L. C. Feldman, V. Podzorov, *Nat. Mater.* **2010**, *9*, 938-943.
- [21] G. M. Akselrod, P. B. Deotare, N. J. Thompson, J. Lee, W. A. Tisdale, M. A. Baldo, V. M. Menon, V. Bulovic, *Nat. Commun.* **2014**, *5*, 3646.
- [22] P. Irkhin, I. Biaggio, *Phys. Rev. Lett.* **2011**, *107*, 017402.
- [23] K. A. Clark, E. L. Krueger, D. A. Vanden Bout, *J. Phys. Chem. Lett.* **2014**, *5*, 2274-2282.
- [24] S. M. Menke, R. J. Holmes, *Energy Environ. Sci.* **2014**, *7*, 499-512.
- [25] O. V. Mikhnenko, P. W. M. Blom, T.-Q. Nguyen, *Energy Environ. Sci.* **2015**, *8*, 1867-1888.
- [26] J. Liu, H. Dong, Z. Wang, D. Ji, C. Cheng, H. Geng, H. Zhang, Y. Zhen, L. Jiang, H. Fu, Z. Bo, W. Chen, Z. Shuai, W. Hu, *Chem. Commun.* **2015**, *51*, 11777-11779.
- [27] W. Zhu, R. Zheng, X. Fu, H. Fu, Q. Shi, Y. Zhen, H. Dong, W. Hu, *Angew. Chem. Int. Ed.* **2015**, *54*, 6785-6789.
- [28] J. Zhang, B. Xu, J. Chen, S. Ma, Y. Dong, L. Wang, B. Li, L. Ye, W. Tian, *Adv. Mater.* **2014**, *26*, 739-745.
- [29] L. Heng, X. Wang, D. Tian, J. Zhai, B. Tang, L. Jiang, *Adv. Mater.* **2010**, *22*, 4716-4720.
- [30] Q. Liao, H. Zhang, W. Zhu, K. Hu, H. Fu, *J. Mater. Chem. C* **2014**, *2*, 9695-9700.
- [31] V. C. Sundar, J. Zaumseil, V. Podzorov, E. Menard, R. L. Willett, T. Someya, M. E. Gershenson, J. A. Rogers, *Science* **2004**, *303*, 1644-1646.
- [32] C. C. Mattheus, A. B. Dros, J. Baas, A. Meetsma, J. L. d. Boer, T. T. M. Palstra, *Acta Crystallogr. Sect. C* **2001**, *57*, 939-941.
- [33] M. Watanabe, Y. J. Chang, S. W. Liu, T. H. Chao, K. Goto, M. M. Islam, C. H. Yuan, Y. T. Tao, T. Shinmyozu, T. J. Chow, *Nat. Chem.* **2012**, *4*, 574-578.
- [34] T. Zhu, Y. Wan, L. Huang, *Acc. Chem. Res.* **2017**, *50*, 1725-1733.
- [35] A. T. Haedler, K. Kreger, A. Issac, B. Wittmann, M. Kivala, N. Hammer, J. Köhler, H.-W. Schmidt, R. Hildner, *Nature* **2015**, *523*, 196.
- [36] D. Shi, V. Adinolfi, R. Comin, M. Yuan, E. Alarousu, A. Buin, Y. Chen, S. Hoogland, A. Rothenberger, K. Katsiev, Y. Losovyj, X. Zhang, P. A. Dowben, O. F. Mohammed, E. H. Sargent, O. M. Bakr, *Science* **2015**, *347*, 519-522.
- [37] X.-H. Jin, M. B. Price, J. R. Finnegan, C. E. Boott, J. M. Richter, A. Rao, S. M. Menke, R. H. Friend, G. R. Whittell, I. Manners, *Science* **2018**, *360*, 897-900.
- [38] W. Zhu, D. Zhang, S. Bai, Q. Shi, W. Hu, H. Fu, *Adv. Opt. Mater.* **2020**, *n/a*, 2000866.

Crystal Matter: We report estimated singlet exciton diffusion length of 124 nm in 2,6-diphenyl anthracene crystals for advanced optoelectronics. The crystals show parallelogram morphology, non-radiation rate constant of 0.26 ns^{-1} , good field-effect transistor hole mobility, and strong electronic couplings. These allow excitons rapidly diffuse to crystal surface for charge separation and bimolecular recombination in photoconductivity experiments.



Weigang Zhu,^{*,+} Yajing Sun,⁺ Jie Liu,
Shuming Bai, Zhicheng Zhang, Qiang
Shi, Wenping Hu,^{*} Hongbing Fu^{*}

Page No. – Page No.

**Exciton Transport in Molecular
Semiconductor Crystals for Spin-
Optoelectronics Paradigm**